

# Live-Cell Imaging of Apoptosis and Necrosis

## Author

Sarah Beckman, PhD  
Agilent Technologies, Inc.

## Abstract

Cell death occurs throughout the life of an organism, and this is critical for developmental plasticity and organismal health, in part by eliminating unneeded and unhealthy cells in a timely and effective manner. However, dysfunctional cell death leads to diseases such as cancer, neurodegeneration, and ischemic damage. This application note investigates apoptosis and necrosis in real time over a 48-hour period using high contrast brightfield imaging in combination with fluorescent probes for apoptotic and necrotic cell death markers. This study demonstrates that apoptosis and necrosis are induced in a dose-dependent manner in both HT-1080 and SKOV3 cells.

## Introduction

Cell death is a vital component of multiple biological processes including normal cell turnover and proper development. Cell death demonstrates a complimentary but opposite role to proliferation in the homeostatic regulation of cellular populations. Inappropriate cell death (either too much or not enough) is a factor in many diseases such as ischemic damage, cancer, and neurodegeneration.<sup>1</sup> Thus, the ability to modulate the life or death of a cell is of immense therapeutic potential.

Two classic pathways of cell death are apoptosis and necrosis. Apoptosis is an active, programmed process of autonomous cellular demise that avoids eliciting an immune response. On the other hand, necrosis is an uncontrolled, passive process which results in the release of inflammatory cytoplasmic content into the surrounding tissue. Critical to each unique cell death pathway is the way in which the resultant cellular debris is cleared. Apoptotic cells display a variety of recognition signals for phagocytes that lead to their expedient removal. The uptake of apoptotic bodies suppresses secretion of inflammatory mediators from activated macrophages. Conversely, the cellular content released from necrotic cells includes molecules that act as signals to promote the inflammatory response.<sup>2</sup>

Despite their differences, apoptosis and necrosis are not mutually exclusive processes. Multiple types of cell death can occur concurrently in cells exposed to the same stimuli. The local intensity, as well as the activation or differentiation state of a particular cell, helps to determine the cell death pathway which is undertaken by each individual cell.<sup>2</sup> Furthermore, the degree of stimuli can determine whether cells die of apoptosis or necrosis. At low doses, a variety of damaging stimuli such as heat, radiation, hypoxia and cytotoxic anticancer drugs can induce apoptosis, but the same stimuli induce necrosis at higher doses.<sup>2</sup>

Quantification of the cell death response is an integral component of exploring cell biology, responses to cellular stress, and performing high-throughput drug screens. Classic methods of cell death detection include flow cytometry, which requires extensive handling of cells and only provides end point data. Kinetic imaging, in contrast, is a critical application for studying dynamic biological processes in real time. Kinetic analysis of cell death allows for sensitive, real-time determination of the accumulation of both apoptotic and necrotic events within the cellular population.

Presented here is the use of apoptosis and necrosis fluorescent probes in combination with automated kinetic imaging to quantitatively assess the effects of known

inducers of cell death in multiple cell lines. Label-free high-contrast brightfield imaging was used to assess the total number of cells and fluorescent probes to quantify concurrently early stage apoptosis at the level of plasma membrane inversion exposing phosphatidyl serine and plasma membrane rupture associated with necrosis. This allows for determination of percent apoptosis and necrosis in each cell population over 48 hours of drug treatment.

## Materials and methods

### Cell culture

HT-1080 cells were grown in Advanced Dulbecco's Modified Eagle's Medium (DMEM) (Gibco, Grand Island, NY) with 10% FBS (Gibco) and 1x PennStrep-Glutamine (Cellgro, Manassas, VA). SKOV3 cells were grown in McCoy's 5a Medium Modified (Gibco) with 10% FBS (Gibco) and 1x PennStrep-Glutamine (Cellgro). Cells were seeded into black sided clear bottom 96-well microplates (Corning, Corning, NY) at a density of 2,000 (HT-1080) or 4,000 (SKOV3) cells per well and were allowed to adhere overnight. Environmental conditions, including temperature (37 °C), gas (5% CO<sub>2</sub>), and humidity (90%) were maintained during the two-day incubation using an Agilent BioTek Biospa 8 automated incubator.

### Cell death induction and component addition

Cell death was induced by treating the cells with dilutions of camptothecin or staurosporine with concentrations ranging from 10,000 to 2.44 nM and a no-compound control. The media also contained reagents from the Kinetic Apoptosis Kit (ab129817), donated by Abcam (Cambridge, MA). The polarity sensitive indicator of viability and apoptosis (pSIVA), a marker of apoptosis, was added to the media at a concentration of 10 µL/mL. Propidium iodide (PI), a necrosis indicator, was added to the media at a concentration of 5 µL/mL.

### Cell imaging

Cell culture plates were transferred by the Agilent BioTek BioSpa 8 to an Agilent BioTek Cytation 5 cell imaging multimode reader every two hours. Environmental conditions were maintained at 37 °C and 5% CO<sub>2</sub> within the Cytation 5 throughout the imaging steps. Images were captured at 4x in the PI, GFP, and brightfield channels. Two high contrast brightfield images were captured at each time point, an in-focus image used for reference, and a defocused image for cell counting. Briefly, cells were brought into focus using the high contrast brightfield kit. The view line profile tool was then used to draw a line that crossed cells and background sections of the imaging field. The focal height was then decreased while observing the line profile to determine

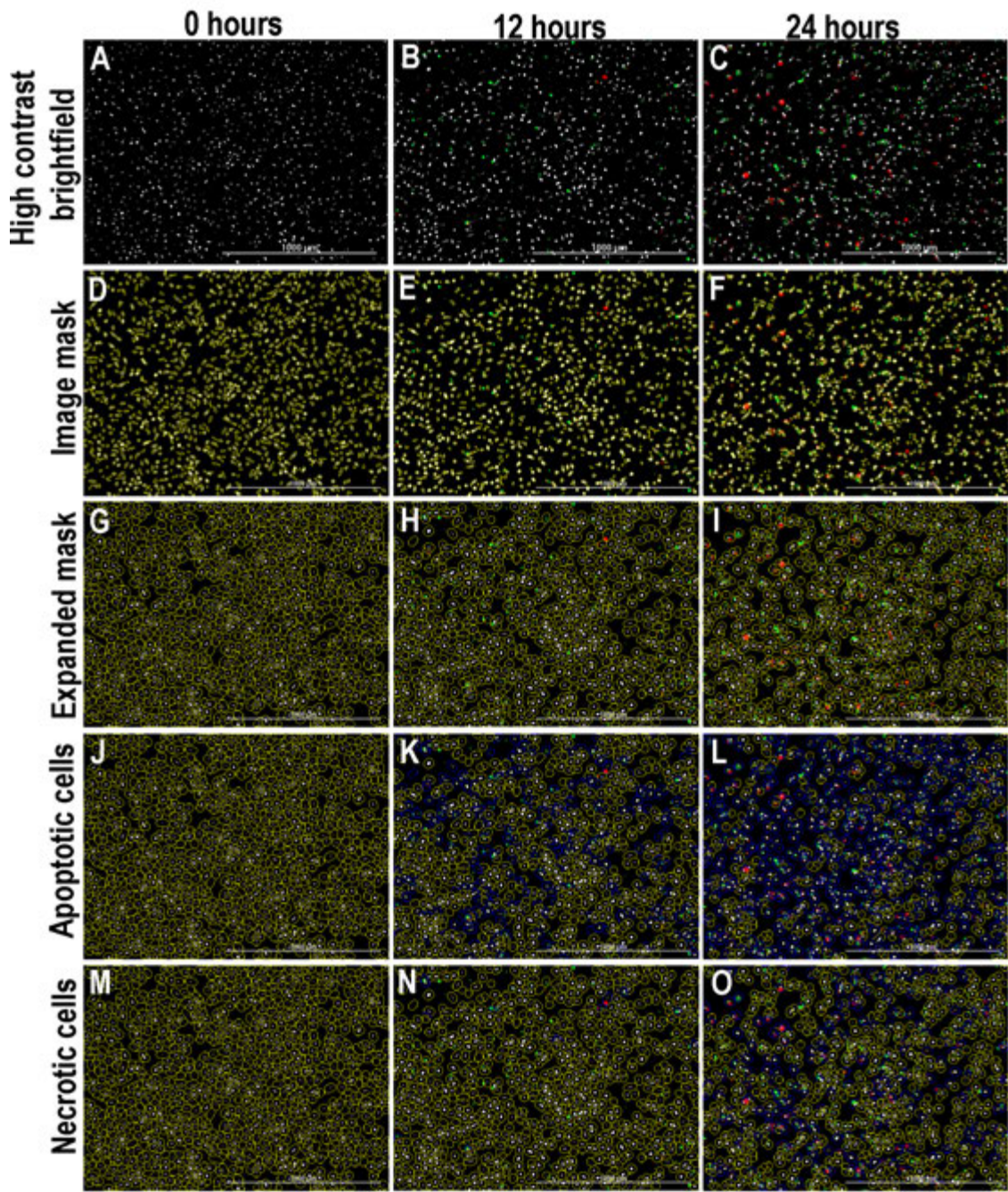
the focal height at which maximum contrast between cell and background brightness was achieved. This value was then input as an offset from the reference high contrast brightfield image.<sup>3</sup>

### Image analysis

Image preprocessing was used to obtain the best possible enhancement of contrast, reducing each cell to a single bright spot. To achieve this, the high contrast image was processed with a black background and a 30 µm rolling ball. This resulted in a dark image with bright spots delineating cells. Automatic background flattening parameters were used to remove background fluorescence from the GFP and PI channels. (Figures 1A to 1C). Object masking thresholds were then set to identify each cell for counting. Images were analyzed by masking on the high contrast brightfield images and expanding the brightfield mask to capture the PI and GFP signal (Figures 1G to 1I). The PI or GFP integral in the secondary mask was calculated for each cell. Image preprocessing and analysis settings are presented in detail in Table 1.

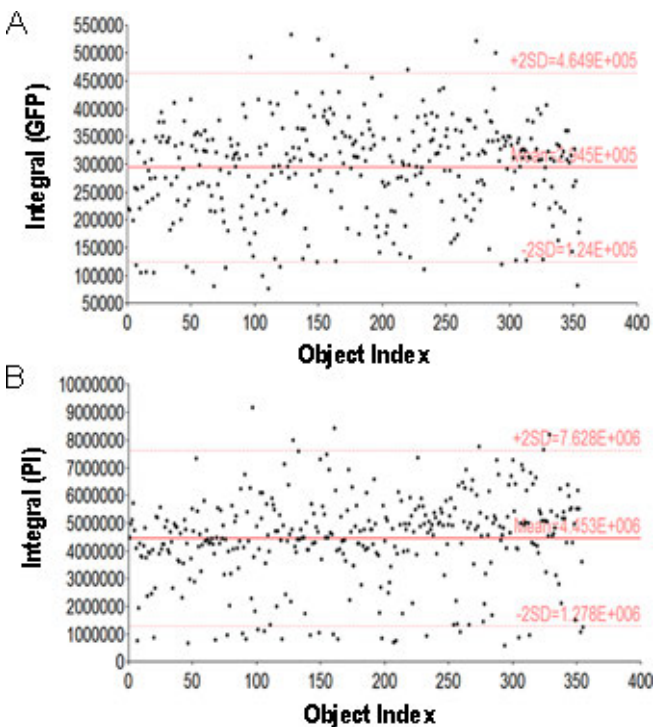
**Table 1.** Agilent BioTek Gen5 microplate reader and imager software settings. Image analysis parameters for generating a cellular mask in the high contrast bright field channel. Primary masks are expanded to encompass the PI and GFP signal to determine the integrals.

Image Preprocessing	
Image Set	Bright Field [2]
Background	Dark
Rolling Bar Diameter	30
Priority	Fine results
Image Smoothing Strength	0
Image Set	Propidium Iodide
Background	Dark
Rolling Bar Diameter	Auto
Image Smoothing Strength	0
Image Set	GFP
Background	Dark
Rolling Bar Diameter	Auto
Image Smoothing Strength	0
Cellular Analysis	
Detection Channel: Primary mask and Count	Tsf[Bright Field [2]]
Threshold	Auto
Background	Dark
Minimum object size	10
Maximum object size	100
Secondary Mask	Tsf[Propidium Iodide]
Measure within a Secondary Mask	Checked
Expand Primary mask	20 µm
Secondary Mask	Tsf[GFP]
Measure within a Secondary Mask	Checked
Expand Primary Mask	30 µm



**Figure 1.** Image analysis of apoptotic and necrotic cells. HT-1080 cells were treated with camptothecin in order to determine the effect of the drug on the apoptotic and necrotic response of HT-1080 cells. The first row (A-C) shows preprocessed high-contrast brightfield images along with GFP and PI at 0 (A), 12 (B), and 24 (C) hours after treatment. The next row of images (D-F) shows the primary mask surrounding each individual cell as delineated by the preprocessed high-contrast brightfield image. Row G-I shows the expanded mask which captures more of the cell area and encompasses the GFP and PI signal. Row J-L shows the apoptotic cells highlighted in blue. Row M-O indicates necrotic cells highlighted in blue.

To determine which cells were positive for apoptosis or necrosis, a threshold was set based upon the negative control well (Figure 2). This threshold was set at 2 standard deviations above the mean of the average value of the negative control well. The percent of total apoptotic/necrotic cells per time point was determined using the ratio transformation function in the data reduction tool box.



**Figure 2.** Scatter plots for apoptosis and necrosis cut-offs. (A) GFP integral and (B) PI integrals from negative control wells were used to determine cutoffs for apoptotic and necrotic cells with subpopulation analysis. The average plus two standard deviations was used as the basis for determining positive apoptotic and necrotic cells.

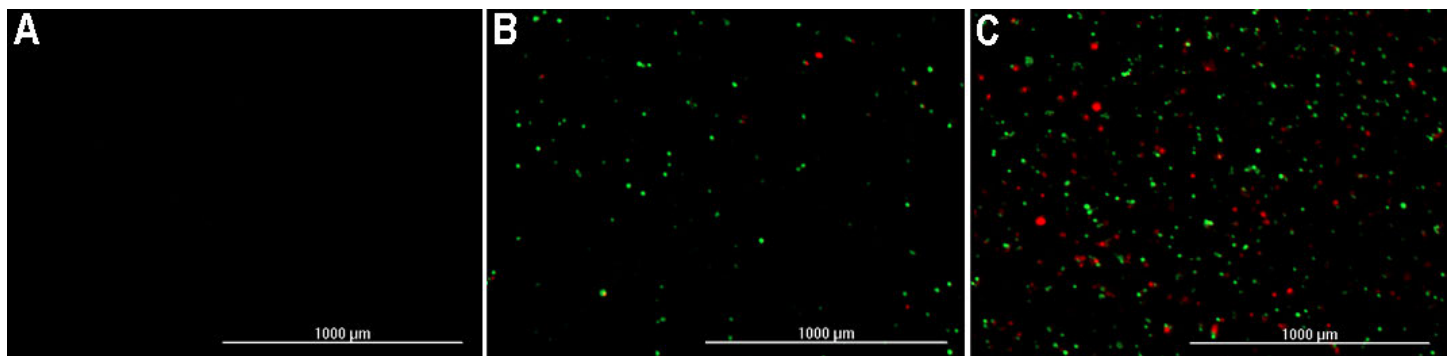


**Figure 3.** Images of HT-1080 cells treated with camptothecin. 4x images at time 0 (A) 12 hours (B) and 24 hours (C) of HT-1080 cells treated with 2,500 nM camptothecin and stained with PI (red, necrosis) and pSIVA (green, apoptosis) are shown. Apoptosis and necrosis both increase over time and these results demonstrate an increase over time in the percentage of GFP positive apoptotic cells and PI positive necrotic cells.

## Results and discussion

One feature of apoptosis is the expression of cell surface markers that result in early phagocytic recognition of apoptotic cells, permitting phagocytosis with minimal compromise to the surrounding tissue. This is achieved by the movement of the normally inward facing phosphatidylserine (PS) of the cell's lipid bilayer to expression on the outer layers of the plasma membrane. Externalization of PS is a well known recognition signal for phagocytes. This study used a probe that binds reversibly to PS, the Polarity Sensitive Indicator of Viability and Apoptosis (pSIVA). A hallmark feature of necrosis is the breakdown of the plasma membrane, allowing uptake of membrane impermeable dyes such as PI, thus indicating the presence of necrotic cells. The pSIVA and PI together act to distinguish between apoptotic and necrotic cell death.

HT-1080 cells were treated with camptothecin to determine the effect of the drug on the apoptotic and necrotic response of HT-1080 cells. Camptothecin is a topoisomerase inhibitor that has high cytotoxicity in a variety of cell lines. Camptothecin acts by binding to the DNA topoisomerase I cleavage complex, which prevents religation of single strand breaks, and causes apoptosis.<sup>4</sup> An increase was found in apoptotic and necrotic cells both over time and according to dose (Figures 3 and 4).

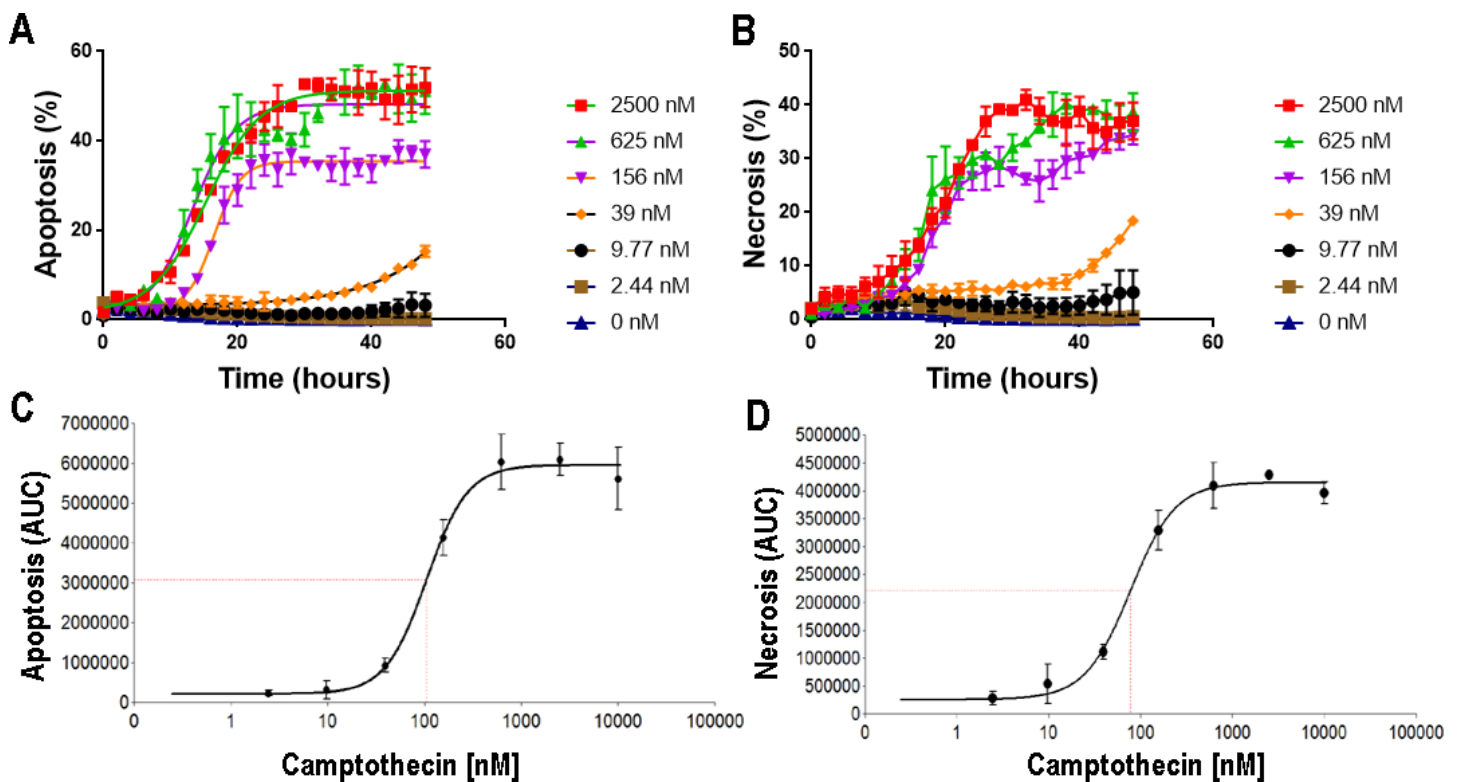


**Figure 4.** HT-1080 cells treated with camptothecin. Apoptosis and necrosis increase in a dose-dependent manner as demonstrated by time course (A,B) and dose response at 48 hours (C,D).

Next, SKOV3 cells were treated with camptothecin to determine the effect of the drug on the apoptotic and necrotic response of SKOV3 cells. Similar to the results with HT-1080 cells, an increase was found in apoptotic and necrotic cells both over time and according to dose (Figure 5). However, looking closely at the two sets of graphs reveals that although both of the cells responded in a time- and dose-dependent manner, there are differences inherent in the responses. In the HT-1080 cells, both apoptosis and necrosis peaked shortly after 24 hours, where in the SKOV3 cells, apoptosis and necrosis climbed more or less steadily after 20 hours, but until then there was little cell death. This is probably due to the fact that SKOV3 cells are known to be resistant to tumor necrosis factor and several cytotoxic drugs.<sup>5</sup> This is a good example of the fact that diverse stimuli are going to affect different cell types in different ways.

HT-1080 cells were treated with staurosporine to determine the effect of the drug on the apoptotic and necrotic response of HT-1080 cells. Staurosporine is a potent protein kinase inhibitor that induces apoptosis in many cell types.<sup>6</sup> In general, an increase was found in apoptotic and necrotic cells both over time and according to dose (Figure 6). However, in the case of necrosis induction at the highest doses, there is a sharp peak at 12 hours which then falls off as the nuclear DNA bound to the PI is lost from the cell and diffuses away from the image plane.

Finally, SKOV3 cells were treated with staurosporine to determine the effect of the drug on the apoptotic and necrotic response of SKOV3 cells. Similar to previous results, an increase was found in apoptotic and necrotic cells both over time and according to dose (Figure 7). However, compared to the response of SKOV3 cells to camptothecin, when exposed to staurosporine, there was a slightly greater overall apoptotic and necrotic response, highlighting the fact that the same cells respond differently to different stimuli.

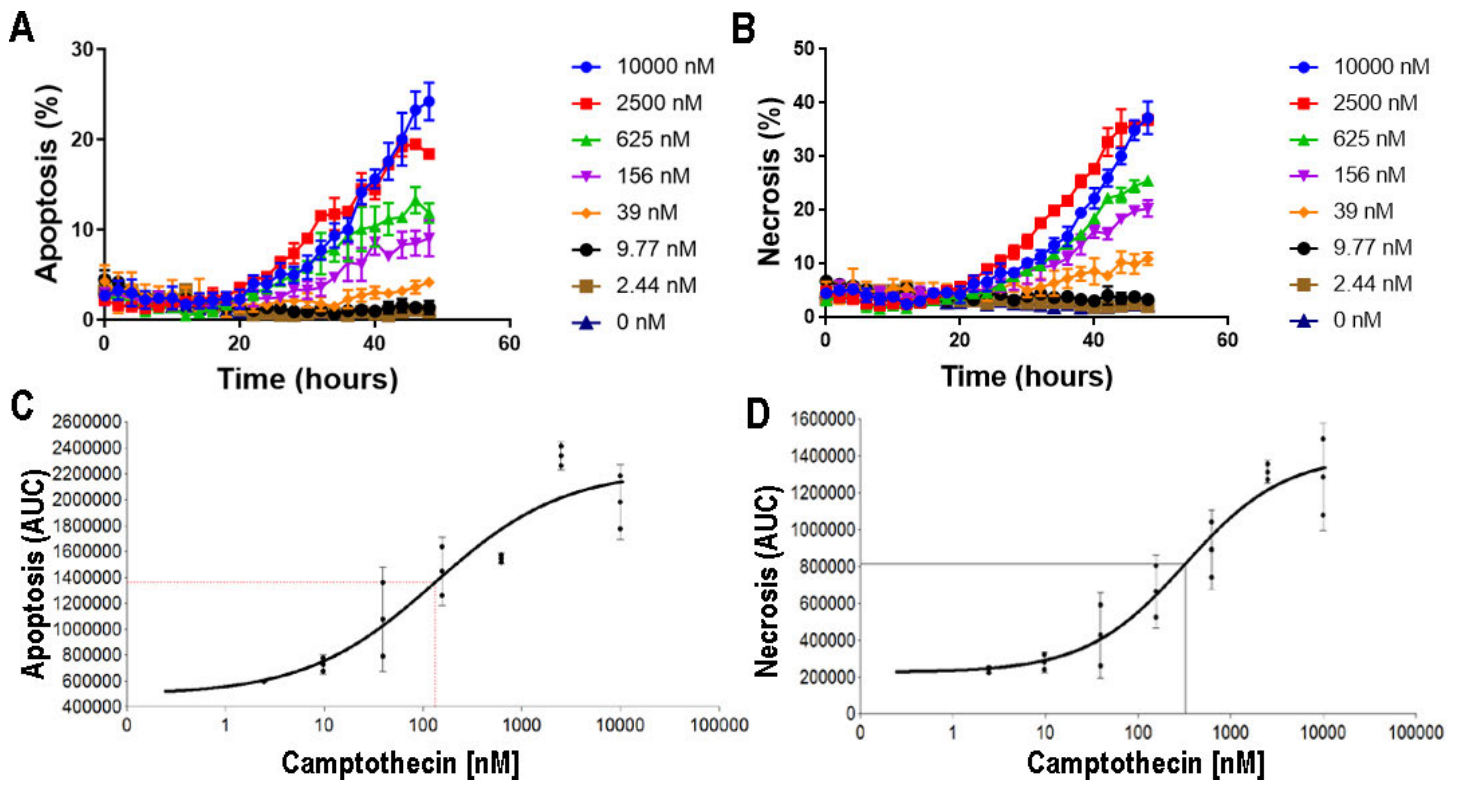


Figure 5. SKOV3 cells treated with camptothecin. Apoptosis and necrosis increase in a dose-dependent manner as demonstrated by time course (A,B) and dose response at 48 hours (C,D).

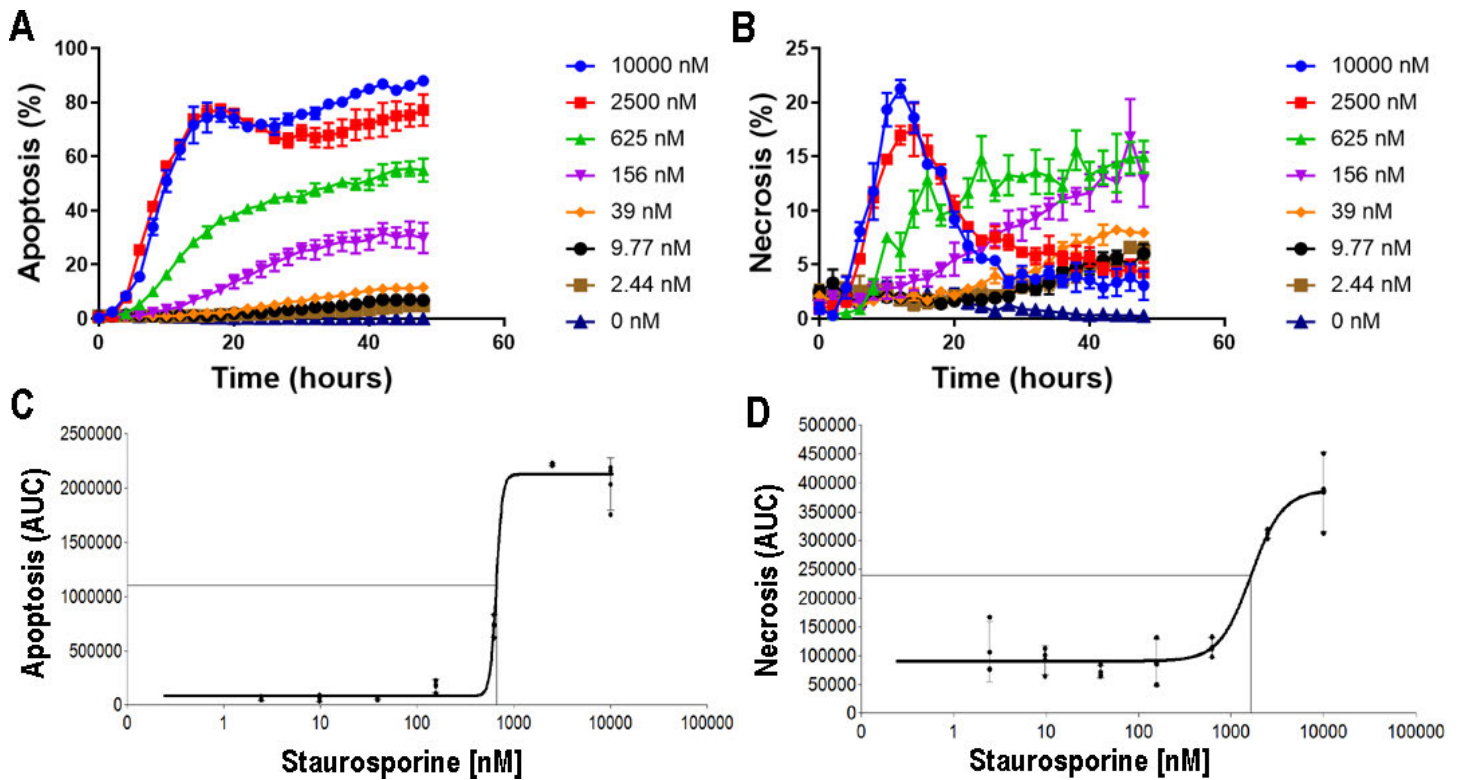
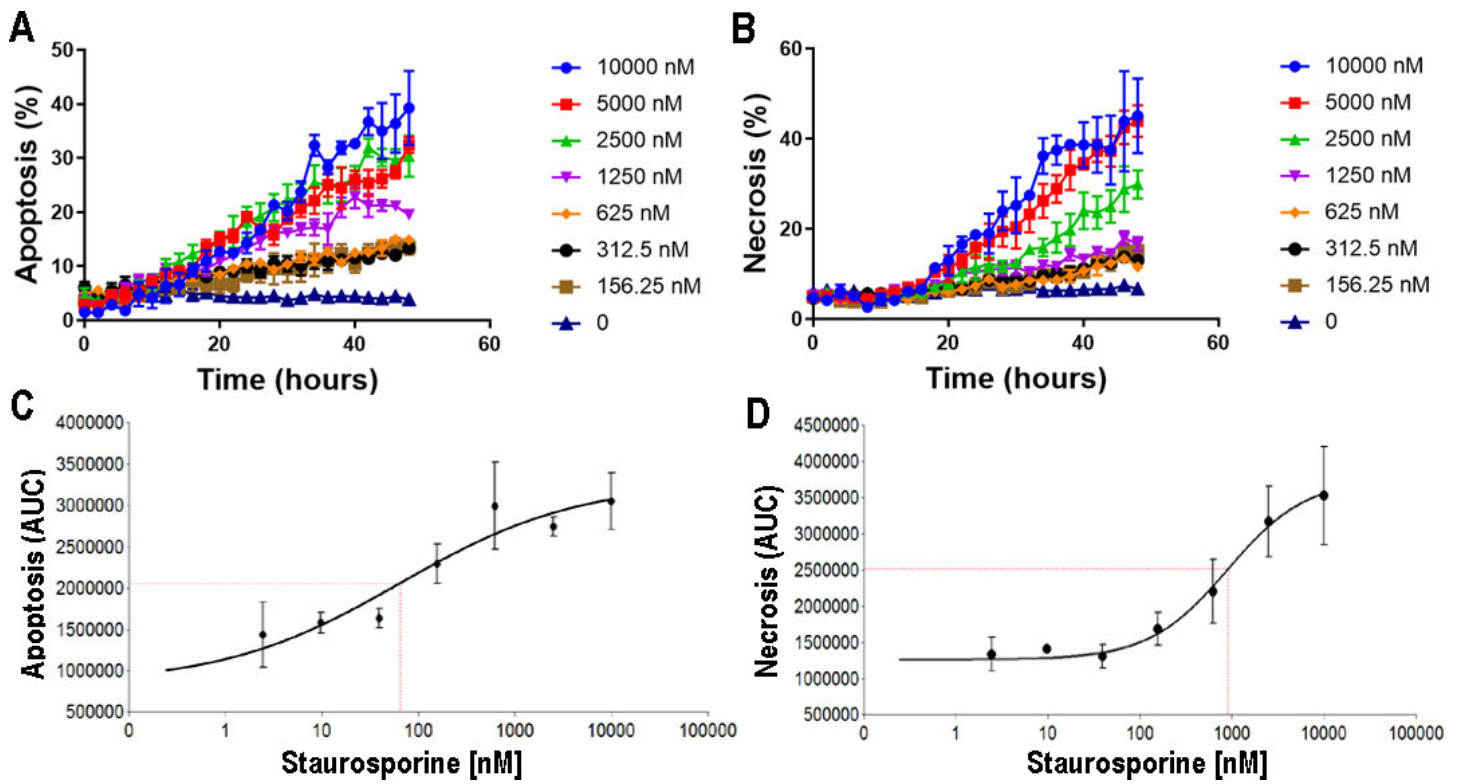


Figure 6. HT-1080 cells treated with staurosporine. Apoptosis and necrosis increase in a dose-dependent manner as demonstrated by time course (A,B) and dose response at maximum levels of cell death at 16 (C) and 12 (D) hours.



**Figure 7.** SKOV3 cells treated with staurosporine. Apoptosis and necrosis increase in a dose-dependent manner as demonstrated by time course (A,B) and dose response at 48 hours (C,D).

## Conclusion

The use of apoptosis and necrosis fluorescent probes in combination with automated kinetic imaging allows quantitative assessment of the effects of known inducers of cell death in multiple cell lines. This assay uses high contrast label-free brightfield imaging to assay for total number of cells and cellular dyes to label both apoptotic and necrotic cells concurrently. This allows the determination of percent apoptosis and necrosis in each cell population over long term drug treatment without use of a nuclear dye. When HT-1080 or SKOV3 cells are treated with dilutions of camptothecin or staurosporine, apoptosis and necrosis are induced in a dose-dependent manner over time. This assay also demonstrates the differing response of different cells to the same stimulus, as in the case of SKOV3 and HT-1080 responding differently to camptothecin. Kinetic analysis of cell death allows sensitive, real-time determination of the accumulation of both apoptotic and necrotic events within the cellular population.

## References

1. Elmore, S. Apoptosis: a Review Of Programmed Cell Death. *Toxicol. Pathol.* **2007**, *35*, 495–516.
2. Fink, S. L. & Cookson, B. T. Apoptosis, Pyroptosis, And Necrosis: Mechanistic Description Of Dead And Dying Eukaryotic Cells. *Infect. Immun.* **2005**, *73*, 1907–16.
3. Clayton, J. Kinetic Proliferation Assay Using Label-Free Cell Counting, **2017**.
4. Venditto, V. J. & Simanek, E. E. Cancer Therapies Utilizing the Camptothecins: a Review of The *In Vivo* Literature. *Mol. Pharm.* **2010**, *7*, 307–49.
5. Morimoto, H., Safrit, J. T. & Bonavida, B. Synergistic Effect of Tumor Necrosis Factor-Alpha- and Diphtheria Toxin-Mediated Cytotoxicity In Sensitive and Resistant Human Ovarian Tumor Cell Lines. *J. Immunol.* **1991**, *147*, 2609–16.
6. Tamaoki, T. *et al.* Staurosporine, a Potent Inhibitor of Phospholipid/Ca<sup>++</sup>-Dependent Protein Kinase. *Biochem. Biophys. Res. Commun.* **1986**, *135*, 397–402.

[www.agilent.com/lifesciences/biotek](http://www.agilent.com/lifesciences/biotek)

For Research Use Only. Not for use in diagnostic procedures.

RA44175.3028935185

This information is subject to change without notice.

© Agilent Technologies, Inc. 2018, 2021  
Printed in the USA, February 1, 2021  
5994-2685EN  
AN032218\_05